J Neurophysiol 108: 3253–3263, 2012.
First published September 19, 2012; doi:10.1152/jn.00606.2012.

Dynamic modulation of intrinsic functional connectivity by transcranial direct current stimulation

Bernhard Sehm,[1,2]* Alexander Schäfer,[1]* Judy Kipping,[1] Daniel Margulies,[1] Virginia Conde,[1] Marco Taubert,[1] Arno Villringer,[1,2] and Patrick Ragert[1]

[1]*Department of Neurology, Max Planck Institute for Human Cognitive and Brain Sciences, Leipzig, Germany; and* [2]*Clinic for Cognitive Neurology, University of Leipzig, Leipzig, Germany*

Submitted 16 July 2012; accepted in final form 19 September 2012

Sehm B, Schäfer A, Kipping J, Margulies D, Conde V, Taubert M, Villringer A, Ragert P. Dynamic modulation of intrinsic functional connectivity by transcranial direct current stimulation. *J Neurophysiol* 108: 3253–3263, 2012. First published September 19, 2012; doi:10.1152/jn.00606.2012.—Transcranial direct current stimulation (tDCS) is a noninvasive brain stimulation technique capable of modulating cortical excitability and thereby influencing behavior and learning. Recent evidence suggests that bilateral tDCS over both primary sensorimotor cortices (SM1) yields more prominent effects on motor performance in both healthy subjects and chronic stroke patients than unilateral tDCS over SM1. To better characterize the underlying neural mechanisms of this effect, we aimed to explore changes in resting-state functional connectivity during both stimulation types. In a randomized single-blind crossover design, 12 healthy subjects underwent functional magnetic resonance imaging at rest before, during, and after 20 min of unilateral, bilateral, and sham tDCS stimulation over SM1. Eigenvector centrality mapping (ECM) was used to investigate tDCS-induced changes in functional connectivity patterns across the whole brain. Uni- and bilateral tDCS over SM1 resulted in functional connectivity changes in widespread brain areas compared with sham stimulation both during and after stimulation. Whereas bilateral tDCS predominantly modulated changes in primary and secondary motor as well as prefrontal regions, unilateral tDCS affected prefrontal, parietal, and cerebellar areas. No direct effect was seen under the stimulating electrode in the unilateral condition. The time course of changes in functional connectivity in the respective brain areas was nonlinear and temporally dispersed. These findings provide evidence toward a network-based understanding regarding the underpinnings of specific tDCS interventions.

centrality; graph-based analysis; noninvasive brain stimulation; primary sensorimotor cortex; resting-state fMRI

TRANSCRANIAL DIRECT CURRENT stimulation (tDCS) is a noninvasive brain stimulation technique known to modulate cortical excitability in a polarity-specific manner (Nitsche et al. 2008). For example, anodal tDCS applied over the primary sensorimotor cortex (SM1) increases corticospinal excitability even beyond the stimulation period, whereas cathodal tDCS decreases it (Nitsche and Paulus 2000). Studies using excitability measurements of the living human brain with transcranial magnetic stimulation (TMS) as well as pharmacological interventions suggested that an increase of excitability induced by anodal stimulation and a decrease of excitability induced by cathodal stimulation depend on changes in the neuronal membrane potential (Nitsche et al. 2003a, 2005). More specifically, anodal tDCS has been shown to result in a depolarization while cathodal stimulation leads to a hyperpolarization of the resting membrane potential. Furthermore, at least for anodal stimulation, a study using magnetic resonance spectroscopy provided evidence that anodal tDCS leads to locally reduced GABA while cathodal stimulation causes reduced glutamatergic neuronal activity with a highly correlated reduction in GABA (Stagg et al. 2009).

In light of these findings, the application of tDCS has reemerged in the last decade as a tool to effectively modulate brain function. Until now, behavioral effects of tDCS have been extensively studied in motor control and motor learning (for review, see Reis et al. 2008). For example, anodal tDCS delivered over SM1 has been consistently shown to transiently improve performance and/or learning of various motor tasks in both healthy subjects (Nitsche et al. 2003c; Stagg et al. 2011) and chronic stroke patients (Hummel et al. 2005; Lindenberg et al. 2010). Furthermore, when applied in multiple sessions on 5 consecutive days, long-term improvements in a sequential pinch force task for up to 3 mo were observed (Reis et al. 2009). These results, together with findings in animal studies showing that tDCS acts upon brain-derived neurotrophic factor (BDNF)-dependent synaptic plasticity, further strengthen its potential as an adjuvant tool in neurorehabilitation (Fritsch et al. 2010).

One important yet open question relates to the optimal arrangement of the tDCS electrodes in order to achieve maximum stimulation effects. In the motor domain, a commonly used tDCS setup consists of a unilateral anodal tDCS electrode over SM1 contralateral to the moving/learning extremity (unilateral tDCS), while the other electrode is applied to the contralateral supraorbital region. More recently, a new tDCS electrode arrangement, which uses simultaneous anodal tDCS of one SM1 and cathodal tDCS of the homologous SM1 (bilateral tDCS), yielded more prominent behavioral effects in healthy subjects during a finger sequence task (Vines et al. 2008) and led to an improvement of the motor deficit in chronic stroke patients (Lindenberg et al. 2010). The more powerful effects of bilateral tDCS over SM1 have been assumed to be related to a more pronounced interference with interhemispheric information processing compared with unilateral tDCS over SM1 (Vines et al. 2008). However, the exact underlying neural mechanisms still remain elusive and certainly require further investigation.

The concurrent use of neuroimaging techniques such as functional magnetic resonance imaging (fMRI) and noninvasive brain stimulation has the potential to uncover neural

* B. Sehm and A. Schäfer made equal contributions to this work.
Address for reprint requests and other correspondence: B. Sehm, Max Planck Inst. for Human Cognitive and Brain Sciences, Dept. of Neurology, Stephanstr. 1a, D-04103 Leipzig, Germany (e-mail: sehm@cbs.mpg.de).

mechanisms of both uni- and bilateral SM1 tDCS effects as proposed for concurrent TMS and fMRI (see Bestmann et al. 2008 for review). Likewise, a number of studies have investigated tDCS-induced changes of functional activation with both fMRI and positron emission tomography during performance of a motor task (Antal et al. 2011; Baudewig et al. 2001; Holland et al. 2011; Kwon and Jang 2011; Lang et al. 2005; Venkatakrishnan and Sandrini 2012). Unlike task-evoked fMRI changes, resting-state fMRI (rs-fMRI) measures spontaneous fluctuations of the BOLD signal in the absence of task engagement. These fluctuations are not random but temporally coherent, thus providing a measure of the brain's intrinsic functional architecture (Fox and Raichle 2007). Recently, a longitudinal learning study provided compelling evidence that patterns of rs-fMRI are persistently modulated by a complex motor skill training over several weeks (Taubert et al. 2011). Furthermore, with the use of unilateral tDCS over SM1, it was demonstrated that rs-fMRI measurements (pre-post design) are capable of depicting tDCS-induced aftereffects on functional connectivity (Pena-Gomez et al. 2012; Polania et al. 2011b).

In the present study, we aimed to investigate changes in intrinsic functional connectivity elicited by both unilateral and bilateral tDCS over SM1 during and after stimulation without any task engagement. Only recently, a first proof-of-concept study validated the technical feasibility of concurrent tDCS and rs-fMRI measurements (Alon et al. 2011). Here the authors investigated changes in functional connectivity between both SM1, using a region of interest approach during short blocks of anodal tDCS (7 min) over right SM1. Despite a highly variable response to tDCS, most likely due to the small sample size of five subjects, the aforementioned study revealed a decrease in functional connectivity from the right to the left SM1 during tDCS.

In this study we aimed at extending these findings by various important factors. First, we aimed at tracking changes in functional connectivity during the course of 20 min of tDCS. This stimulation duration has been most commonly used in studies of motor behavior and learning (Reis et al. 2009; Vines et al. 2008). Second, in order to obtain information regarding potential aftereffects of the stimulation, we continued scanning for a further ~15 min. Third, we compared two different stimulation setups (bilateral and unilateral tDCS over SM1) with sham stimulation to better understand the neurophysiological underpinnings. Fourth, we aimed at investigating the effects of both stimulation approaches on large-scale brain networks by using eigenvector centrality mapping (ECM). ECM is a graph-based measure for centrality in functional brain networks that attributes a value to each voxel in the brain such that a voxel receives a large value if it is strongly correlated with many other nodes that are themselves central within the network. Thus it allows for the exploratory tracking of changes in network architecture across the whole brain (Lohmann et al. 2010; Zuo et al. 2012).

Using this experimental setup, we tested the hypothesis that bilateral and unilateral tDCS over SM1 relative to sham stimulation result in differential time-dependent engagements of intrinsic functional connectivity networks in human subjects.

METHODS

Subjects. We enrolled a total of 12 healthy young volunteers in the study (mean ± SD age 25.8 ± 3.2 yr; 4 women, 8 men). All subjects gave written informed consent to participate in the experiment according to the Declaration of Helsinki, and the ethics committee of the University of Leipzig approved the study. Prior to participation, all subjects underwent a comprehensive neurological examination to screen for potential exclusion criteria. They were not taking any medication. Subjects that did not meet the protocol criteria and/or had contraindications for tDCS or MRI measurements were excluded from participation. In each subject, handedness was assessed based on the Edinburgh Handedness Inventory (Oldfield 1971). Patients reported their hand preference (i.e., right, left, or ambidextrous) in response to 10 questions (e.g., Which hand do you use to light a match? Use scissors? Write?). Responses to the 10 questions were converted to a laterality quotient (LQ) with the formula $(R - L)/(R + L) \times 100$. LQ scores thus might range from −100 (corresponding to strong left-handedness) to +100 (corresponding to strong right-handedness). For our study, only moderately to strongly right-handed subjects, e.g., subjects with an LQ of at least +60 (92.08 ± 11.64; mean ± SD) were included (see, e.g., Isaacs et al. 2006).

Experimental design. Each subject participated in a total of three sessions that comprised concurrent tDCS over SM1 and rs-fMRI in a crossover design. The only difference between each session was the type of tDCS: unilateral tDCS (with the anode placed over the right SM1 and the cathode placed over the contralateral orbit), bilateral tDCS (with anodal stimulation of right and cathodal stimulation of left SM1), or sham stimulation (here, the setup of the unilateral or bilateral tDCS condition was randomly chosen). The order of the sessions was randomized between and within subjects. Sessions were separated by at least 1 wk to avoid any carryover effects.

Transcranial direct current stimulation. tDCS was delivered by a battery-driven DC current stimulator (Neuroconn, Ilmenau, Germany) with a pair of electrodes in a 5 × 7-cm saline-soaked sponge. The electrodes were manufactured to be compatible with the MR scanner environment (Neuroconn) and equipped with ~5-kΩ resistors in each wire to avoid sudden temperature increases due to induction currents from radio frequency pulses, as described previously (Antal et al. 2011). The electrode cables ran through the MR room and passed a radio frequency filter in the MR cabin wall in order to reduce potential artifacts during image acquisition. The cables were connected to a MR-compatible DC stimulator that was placed outside the scanner room. Two filter boxes (Neuroconn) were placed between electrodes and stimulator.

Before MRI scanning, the electrodes were attached to the subject's head with elastic bands. We deployed different electrode montages for each session in accordance with a previously published study (Vines et al. 2008). For unilateral right SM1 stimulation, the anode was centered over C4 according to the International 10-20 System while the cathode was attached to the forehead above the contralateral orbit. For bilateral SM1 stimulation, the anode was centered over C4 (corresponding to right SM1) while the cathode was centered over C3 (corresponding to the left SM1; see also Fig. 1*A*).

For all experimental conditions (unilateral and bilateral tDCS over SM1 and sham stimulation), the current was increased in a ramplike fashion over the first 30 s of stimulation to a maximum of 1 mA, eliciting a transient tingling sensation on the scalp. tDCS was delivered for 20 min in the uni- and bilateral tDCS conditions and for up to 30 s in the sham stimulation condition. During stimulation, a continuous monitoring of the impedance revealed no changes throughout the experiment. The current density at the stimulation electrodes at our maximum setting of 1 mA for uni- and bilateral tDCS over SM1 was 0.028 mA/cm^2. Total charge as expressed by current density × total stimulation duration (s) was 0.034 C/cm^2. Thereafter, currents were turned off slowly over a few seconds, precluding sensory differences between conditions (Nitsche et al. 2003b). This strategy has been shown to be efficient in blinding of the procedure (Gandiga et al. 2006; Ragert et al. 2008).

Scanning protocol. fMRI data were acquired under eyes-closed conditions on a Siemens Magnetom Tim Trio 3 Tesla scanner

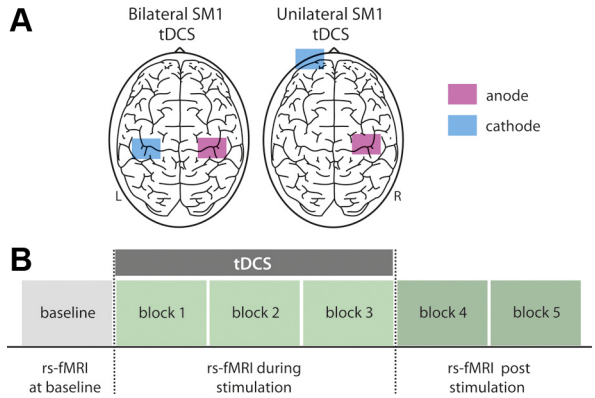

Fig. 1. Experimental setup showing the different electrode montages used (*A*) and the time course of 1 experiment (*B*). *A*: for bilateral transcranial direct current stimulation (tDCS) over primary sensorimotor cortex (SM1), the anode was mounted over the right SM1 while the cathode was mounted over the homologous left SM1. For unilateral SM1 tDCS, the anode was again placed over the right SM1, while the cathode electrode was mounted over the contralateral supraorbital region. *B*: during each experimental session, an initial baseline scan was acquired before tDCS application. Subsequently, the respective tDCS (unilateral, bilateral, or sham SM1 tDCS) was applied for 20 min during the next 3 blocks (total of 600 volumes, duration of ~23 min), followed by 2 additional echo-planar imaging (EPI) blocks (duration of ~15.3 min) that were acquired directly after tDCS. The same procedure applied for the sham stimulation condition except that the tDCS was only applied for ~30 s. For details, see METHODS. rs-fMRI, resting-state fMRI.

equipped with a standard eight-channel head coil. During each session, a total of 6 blocks of echo-planar imaging (EPI) were acquired with 200 whole-brain volumes, each using the following parameters: acquisition matrix = 64 × 64, slice thickness = 3 mm (1-mm gap), voxel dimensions = 3 × 3 × 4 mm, 34 slices, TR = 2,300 ms, TE = 30 ms, flip angle = 90°, bandwidth = 1,825 Hz. The total time for each fMRI session was ~55 min. Before scanning, tDCS electrodes were attached to the scalp of each subject outside of the scanner room (see also tDCS procedures above). Subsequently, subjects were brought into the scanner room, and one EPI sequence (duration ~7.6 min) was acquired before tDCS application (rs-fMRI at baseline). Subsequently, the respective tDCS condition (unilateral, bilateral, or sham tDCS over SM1) was started and applied for 20 min for the *verum* conditions during the next three blocks (total of 600 volumes, duration of ~23 min) followed by two additional EPI blocks (total of 400 volumes, duration of ~15.3 min) that were acquired directly after the stimulation (also see Fig. 1*B*). The same procedure applied for the sham stimulation condition except that the tDCS was only delivered for ~30 s.

Preprocessing and statistical analysis of fMRI data. In brief, as described previously (Lohmann et al. 2010; Taubert et al. 2011), preprocessing of fMRI data was performed with LIPSIA (Lohmann et al. 2001) and included motion correction, band-pass filtering (1/90–1/10 Hz), and spatial smoothing [6-mm full-width half-maximum (FWHM) smoothing]. Preprocessed data sets were registered into standard MNI152 (Montreal Neurological Institute) brain space and resampled to an isotropic voxel grid with a resolution of 3 × 3 × 3 mm. ECM (Lohmann et al. 2010) was used to map changes in network architecture induced by tDCS. ECM is a graph-based method that aims to map the central hubs of functional connectivity networks. ECM specifically weights nodes based on their degree of connection within the network. It does so by counting both the number and the quality of connections so that a node with relatively few connections to some high-ranking other nodes may outrank one with a larger number of mediocre contacts. Google's "PageRank" algorithm is a variant of eigenvector centrality. Compared with other centrality measures, ECM is computationally fast and does not depend on a preselected set of nodes (Zuo et al. 2012). This measure may be applied to all voxels in the brain, thereby avoiding any selection bias. Here we performed voxelwise analyses of rs-fMRI data. This requires in our study a large region of interest of ~63,000 voxels covering the whole brain including the cerebellum, rendering other centrality measures, such as betweenness centrality, computationally intractable (Lohmann et al. 2010). ECM enabled us to obtain whole-brain centrality maps and use them in a manner similar to contrast maps obtained in standard regression analyses. Furthermore, ECM does not depend on a prespecified threshold for correlation values and captures small-world characteristics of the human brain in contrast to other measures such as, e.g., degree centrality (Bonacich 2007; Lohmann et al. 2010). One of the strengths of ECM compared with other related analysis techniques [such as independent component analysis (ICA)] is that ECM captures the centrality of each voxel in a given network while methods such as ICA rather identify subnetworks on a whole-brain level. Thus only voxels changing their network association would be identified with ICA analyses. In light of this knowledge, we decided to use ECM instead of ICA in the present study.

Changes in eigenvector centrality of functional connectivity are described as "eigenvector centrality changes" or "centrality changes in functional connectivity" for the sake of simplicity throughout the text.

After preprocessing, single-subject eigenvector centrality maps were computed for each condition (bilateral, unilateral, and sham SM1 stimulation) and each scanning block (baseline, *blocks 1–5*). Subsequently, ECM maps were used for group-level analysis using general linear regression. z-Maps were thresholded at $z > 3.3$ on a voxel level. Furthermore, corrections for multiple comparisons were implemented at the cluster level with alphasim (cluster significance $P < 0.05$, corrected), which is a cluster size-based Monte Carlo simulation (Forman et al. 1995).

Changes in eigenvector centrality during stimulation were analyzed as follows: z-Maps of the stimulation period (e.g., average of *blocks 1*, *2*, and *3*; refer to Fig. 1*B*) were contrasted against baseline for each condition separately and compared with sham stimulation, in line with a recently published study (Keeser et al. 2011): (bilateral > baseline) > (sham > baseline); (unilateral > baseline) > (sham > baseline).

In a next step, we performed an additional linear regression analysis (see above) comparing differences in eigenvector centrality between bilateral and unilateral tDCS over SM1 during stimulation (*blocks 1–3*): (bilateral > baseline) > (unilateral > baseline); (unilateral > baseline) > (bilateral > baseline).

The aftereffects of the stimulation on eigenvector centrality were analyzed in a similar way by averaging *blocks 4* and *5* contrasted with baseline for both conditions (bi- and unilateral tDCS over SM1) relative to sham stimulation. Subsequently, we performed stepwise comparisons for each block (*blocks 1–5*) against baseline compared with sham stimulation in order to detect potential dynamic changes in eigenvector centrality over time.

As an additional analysis step, differences in eigenvector centrality between stimulation conditions at baseline were analyzed by contrasting the baseline block of each condition (sham, unilateral, bilateral tDCS over SM1) with each other: baseline (sham) vs. baseline unilateral; baseline sham vs. baseline bilateral; baseline unilateral vs. baseline bilateral.

RESULTS

Differences in eigenvector centrality between conditions at baseline. First, we performed baseline comparisons between conditions (bilateral, unilateral, and sham tDCS over SM1). This analysis revealed differences in eigenvector centrality between the three stimulation conditions in several subcortical and cortical areas (Fig. 2).

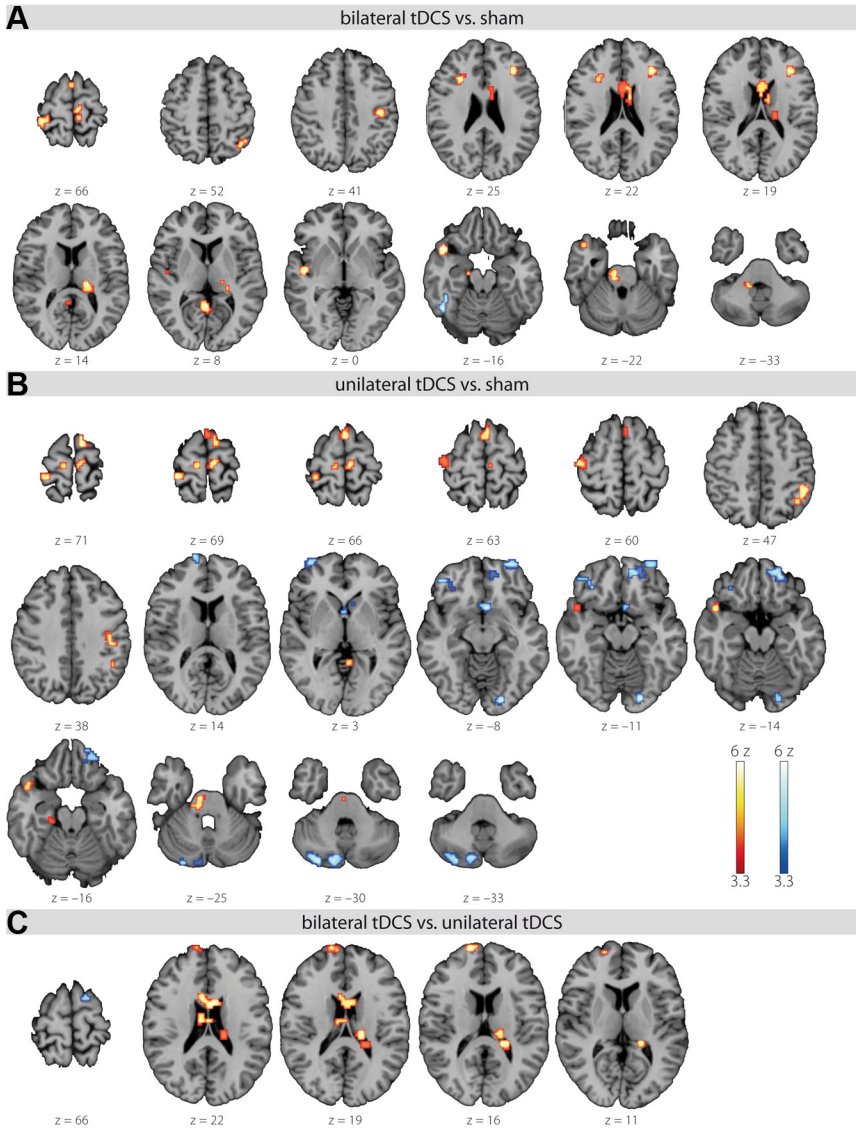

Fig. 2. Baseline comparisons between conditions (bilateral, unilateral, and sham SM1 tDCS). *A*: significant clusters of the comparison bilateral > sham are displayed in red and the inverse contrast (sham > bilateral) in blue. *B*: significant clusters of the comparison unilateral > sham are displayed in red and the inverse contrast (sham > unilateral) in blue. *C*: significant clusters of the comparison bilateral > unilateral are displayed in red and the inverse contrast (unilateral > bilateral) in blue. For the analysis, only the 1st scanning block (baseline, see Fig. 1) of each condition was used. All clusters are presented on axial slices at a threshold of $z > 3.3$ ($P < 0.05$, corrected on cluster level).

Changes in eigenvector centrality during bi- and unilateral SM1 stimulation. Twenty minutes of bilateral tDCS over SM1 (*blocks 1–3*) resulted in increased eigenvector centrality in networks that included motor-related regions such as right primary motor cortex (M1), dorsal premotor cortex (PMd), and bilateral supplementary motor area (SMA) compared with sham stimulation. Furthermore, prefrontal regions were also modulated, such as right superior frontal gyrus (SFG), inferior frontal gyrus (IFG), and left middle frontal gyrus (MFG).

In contrast, during unilateral tDCS only left fronto-temporal and bilateral parietal areas showed a significantly increased centrality in functional connectivity compared with sham stimulation. Furthermore, we found an increase within the right cerebellum (lobule VIIa), ipsilateral to the site of stimulation ($P < 0.001$, corrected; see Fig. 3 and Table 1). Interestingly, no change in eigenvector centrality was found in the cortical area below the stimulating tDCS electrode: the right SM1.

Differential effects on eigenvector centrality during bi- and unilateral SM1 stimulation. A direct comparison between eigenvector centrality changes during 20 min of bi- and unilateral tDCS over SM1 (*blocks 1–3*) revealed differential effects between stimulation types. Bilateral tDCS over SM1 resulted in significantly larger eigenvector centrality changes predominantly in primary and secondary motor areas (including right M1, PMd, and left SMA/pre-SMA), bilateral prefrontal areas (SFG), and subcortical regions compared with unilateral tDCS over SM1. On the other hand, unilateral compared with bilateral tDCS over SM1 resulted in significantly larger increases in right prefrontal (SFG), left parieto-temporal, and subcortical areas including the globus pallidum ($P < 0.001$, corrected, see Fig. 4; for details see Table 2).

Aftereffects of uni- and bilateral stimulation over SM1 on eigenvector centrality. After bilateral tDCS over SM1 (*blocks 4* and *5*), we observed an increase of centrality in functional connectivity in motor-related brain regions such as right M1, PMd, as well as bilateral SMA. Since these regions also showed a significant modulation during stimulation, this result indicates that the increase in eigenvector centrality in these regions persisted for at least 15 min after termination of stimulation. Furthermore, we observed additional alterations in bilateral prefrontal areas that developed after the stimulation period ($P < 0.001$, corrected; see also Table 3 and Fig. 5).

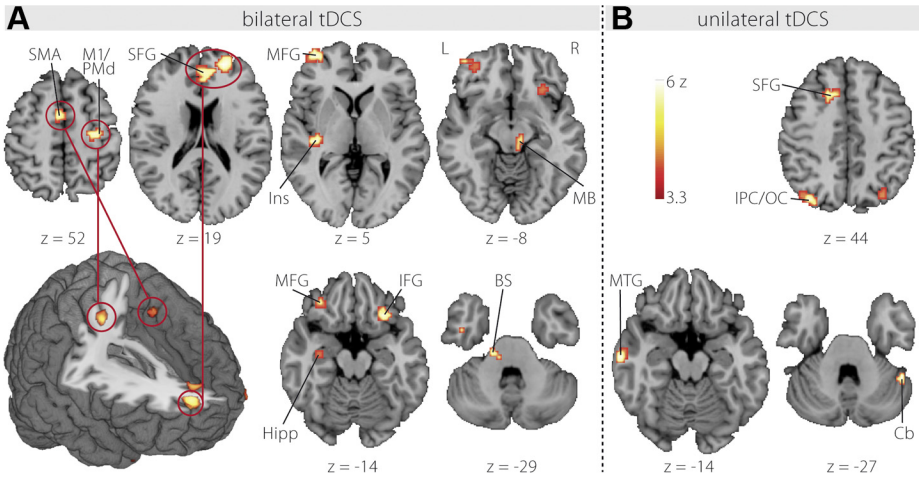

Fig. 3. Brain areas that showed a significant increase in eigenvector centrality during bilateral tDCS over SM1 (*A*) and unilateral tDCS over SM1 (*B*) compared with sham stimulation. Significant clusters are presented on axial slices at a threshold of $z > 3.3$ ($P < 0.05$, corrected on cluster level). Color bars indicate z score in a range of 3.3–6. M1/PMd, primary motor cortex/dorsal premotor cortex; SMA, supplementary motor area; SFG, superior frontal gyrus; MFG, middle frontal gyrus; Ins, posterior insula; MB, midbrain; IFG, inferior frontal gyrus; Hipp, hippocampus; BS, brain stem; IPC/OC, inferior parietal/occipital cortex; MTG, middle temporal gyrus; Cb, cerebellum lobule VIIa hemisphere.

After unilateral tDCS (*blocks 4* and *5*) we observed an increase of eigenvector centrality within the right prefrontal cortex, left middle temporal lobe, right fusiform and middle temporal gyrus, as well as bilateral cerebellum ($P < 0.001$, corrected). See Table 3 for a detailed list of all clusters as well as Fig. 5.

Stepwise comparison of stimulation-induced connectivity changes over time versus baseline. We further assessed changes in eigenvector centrality in each single scanning block (see Fig. 1) compared with baseline, which in turn enabled us to continuously track changes over time, e.g., during (*blocks 1–3*) as well as after (*blocks 4* and *5*) tDCS (for an overview refer to Fig. 6). As described above, bilateral and unilateral tDCS over SM1 resulted in a differential modulation of neuronal networks both during and after stimulation. Moreover, we observed diverse, nonlinear patterns of changes in centrality of functional connectivity within different brain areas over time (see Fig. 6). For example, the bilateral SM1 tDCS condition resulted in a significant change in eigenvector centrality within the cluster of right M1 during the first stimulation block compared with baseline. This effect decreased in *blocks 2* and *3* and subsequently increased again in *blocks 4* and *5* (after stimulation). In contrast, we observed a different pattern over time within right SFG. Here, a steady increase in eigenvector centrality during bilateral SM1 tDCS (*blocks 1–3*) was followed by a decrease after termination of stimulation. Similar diverse patterns are observed in other brain areas for uni- as well as bilateral SM1 tDCS as shown in Fig. 6. In general, these results disclose a temporally and spatially dispersed nonlinear pattern of tDCS-induced centrality changes of whole-brain functional connectivity for both conditions.

Table 1. *Brain regions that show significant increases in eigenvector centrality during bilateral and unilateral tDCS over SM1 compared with sham stimulation*

Brain Area	H	BA	Coordinates (tal)			z Max	Cl
			x	*y*	*z*		
Bilateral tDCS							
M1/PMd	R	4/6	26	−18	49	4.95	837
SMA	L	6	−3	0	52	4.34	486
anterior SFG	R	10	20	51	19	6	3,726
MFG	L	10	−38	57	5	4.99	1,161
		11	−35	48	−11	3.95	621
IFG (p. orbit.)	R	47	26	24	−14	5.54	1,080
Posterior insula	L	13	−38	−24	3	5.72	756
Midbrain	R		9	−24	−8	4.42	459
Hippocampus	L		−32	−12	−19	4.82	648
Brain stem	L		−17	−21	−25	4.41	513
Unilateral tDCS							
SFG	L	8	−17	18	44	4.32	459
IPC/OC	L	19/39	−35	−78	41	5.29	999
IPC/OC	R	19/39	32	−72	38	4.78	783
MTG	L	21	−64	−15	−14	4.92	513
Cb Lob VIIa Hem	R		46	−51	−27	5.02	405

tDCS, transcranial direct current stimulation; SM1, primary sensorimotor cortex; H, hemisphere; BA, Brodmann area; tal, Talairach space; z max, maximum z value; Cl, cluster size; M1, primary motor cortex; PMd, dorsal premotor cortex; SMA, supplementary motor area; SFG, superior frontal gyrus; MFG, middle frontal gyrus; IFG (p. orbit.), inferior frontal gyrus, pars orbitalis; IPC, inferior parietal cortex; OC, occipital cortex; MTG, middle temporal gyrus; Cb, cerebellum.

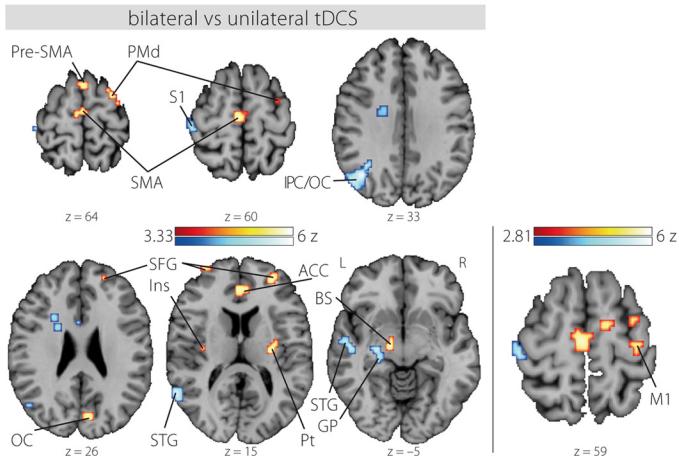

Fig. 4. Differential effects of bilateral vs. unilateral tDCS over SM1 on eigenvector centrality. Bilateral tDCS results in stronger eigenvector centrality increases in primary and secondary motor areas (including right M1, PMd, and left SMA/pre-SMA), bilateral prefrontal areas (SFG), and subcortical regions when directly compared to unilateral SM1 tDCS (bilateral > unilateral tDCS, clusters shown in red). Significant clusters of the inverse contrast (unilateral > bilateral tDCS) are shown in blue. The corrected threshold was set to $z > 3.3$. Color bars indicate z score in a range of 2.8–6 ($P < 0.05$, corrected on cluster level). Pre-SMA, pre-supplementary motor area; Ins, insula; Pt, putamen; S1, primary somatosensory cortex; STG, superior temporal gyrus; GP, globus pallidum.

Table 2. *Differential effects of bilateral and unilateral tDCS over SM1 on eigenvector centrality during stimulation*

Brain Area	H	BA	Coordinates (tal)			z Max	Cl
			x	*y*	*z*		
Bilateral tDCS > unilateral tDCS							
PMd	R	6	26	−12	69	4.29	594
M1	R	4	35	−23	58	3.31	
Pre-SMA	L	6	−3	15	69	4.73	486
SMA	L	6	−3	−18	58	4.87	783
SFG	R	10	29	51	11	4.79	1,458
SFG	L	10	−32	60	16	3.88	945
ACC	L	32	−3	39	14	4.35	783
OFC	R	11	23	30	−16	4.19	432
Insula	L	13	−35	−15	16	4.23	405
OC	R	18	6	−78	25	4.43	486
Putamen	R		29	−15	14	5.13	432
BS	L		−12	−15	−8	5.71	594
Cb Lob VIIb Vermis	L		−3	−72	−25	5.85	837
Unilateral tDCS > bilateral tDCS							
SFG	R	8	17	21	49	4.62	432
S1	L	1	−46	−27	60	4.83	729
IPC/OC	L	39/19	−38	−66	33	5.69	3,267
STG	L	22	−58	−57	14	4.86	1,512
STG	L	22	−52	−12	−3	5.58	1,026
GP	L		−26	−18	−5	4.49	675

ACC, anterior cingulate cortex; OFC, orbitofrontal cortex; BS, brain stem; S1, primary somatosensory cortex; STG, superior temporal gyrus; GP, globus pallidum.

DISCUSSION

Here we provide novel evidence that tDCS over SM1 is capable of modulating functional whole-brain resting-state network connectivity during as well as after stimulation (Zheng et al. 2011). The experimental setup with concurrent tDCS and fMRI allowed us to continuously track tDCS-induced effects on resting-state functional connectivity over time. We showed that bilateral tDCS over SM1 resulted in widespread connectivity changes such as in primary and secondary motor as well as prefrontal cortex. In contrast, unilateral tDCS over SM1 predominantly modulated functional connectivity in prefrontal, parietal, and cerebellar areas. Furthermore, we observed for both stimulation types differential effects not only during but also after tDCS that persisted for at least 15 min. The time course of changes in functional connectivity in the respective brain areas was nonlinear and temporally dispersed.

The combination of noninvasive brain stimulation and modern neuroimaging techniques enables investigation of not only local but also global effects of tDCS on brain networks, e.g., by combining noninvasive brain stimulation and fMRI or EEG measurements (Bestmann et al. 2008; Kirimoto et al. 2011; Neuling et al. 2012). However, until now, only a small number of studies have investigated the effect of noninvasive brain stimulation protocols such as repetitive (r)TMS (e.g., van der Werf et al. 2010) on resting-state networks. Even less is known regarding the effects of tDCS on resting-state functional connectivity. In a first proof of concept on five healthy subjects, the technical feasibility of concurrent tDCS and rs-fMRI measurements could be demonstrated (Alon et al. 2011). Data analysis was restricted to both SM1 (region of interest approach), showing that a decrease in functional connectivity from right to left SM1 was induced by 7 min of anodal tDCS delivered over right SM1. In the present study, we used ECM analysis to identify changes in functional connectivity on a whole-brain level. The use of a centrality measure such as ECM is based on the assumption that important brain regions (hubs) interact with many other regions and facilitate integrative processes (Rubinov and Sporns 2010). The neurobiological interpretation of this measure is that nodes with a high value are interacting functionally with many other nodes in the network. Thus changes in centrality represent reorganizational processes within this functional network architecture.

In contrast to other centrality measures such as betweenness or degree centrality, ECM is parameter free and computationally fast and does not depend on prior assumptions (a priori information) (Lohmann et al. 2010). Previous studies commonly used an anatomical template of 90 regions of interest (Achard et al. 2006; He et al. 2009). However, we aimed to perform voxelwise analysis with our functional data. This required a large region of interest of ~63,000 voxels in our study, which makes measures such as betweenness centrality computationally intractable. The computational speed of ECM enabled us to obtain whole-brain centrality maps and use them in a manner similar to contrast maps obtained in standard regression analyses. Furthermore, in contrast to degree centrality, ECM does not depend on a prespecified threshold for correlation values and captures small-world characteristics of the human brain that degree centrality does not (Bonacich 2007; Lohmann et al. 2010). This method has been used before to detect reorganizational processes in functional connectivity induced by complex motor skill learning (Taubert et al. 2011). In our study, the use of ECM was motivated by findings of concurrent fMRI-TMS experiments showing that noninvasive brain stimulation over SM1 modifies the BOLD signal not only locally within the stimulated or adjacent cortical regions but

Table 3. *Aftereffects of bilateral and unilateral tDCS over SM1 on eigenvector centrality*

Brain Area	H	BA	Coordinates (tal)			z Max	Cl
			x	*y*	*z*		
Bilateral tDCS							
M1/PMd	R	4/6	26	−18	49	5.29	1,809
SMA	R	6	6	−24	66	4.16	621
	L	6	−6	−3	49	4.31	459
	R	6	9	−12	49	4.89	405
Pre-SMA	R	6	3	24	66	4.71	567
MFG	R	9	12	39	33	5.98	7,101
	R	9	43	21	36	4.22	459
OFC	L	11	−23	57	−11	5.1	3,834
IFG (p. orbit.)	R	47	29	24	−19	4.64	459
MTG	R	21	61	−21	−14	5.77	1,134
ITG	L	20	−52	−12	−25	5.24	729
Posterior insula	L		−38	−3	−11	4.18	513
TTG	L	41	−35	−27	8	4.99	594
Cb Lob VIIa Hem	R		38	−75	−27	4.54	702
Unilateral tDCS							
SFG	R	8	20	42	41	5.3	1,971
PHC	L	36	−38	−33	−8	5.43	2,430
FG	R	19	35	−66	−5	4.38	540
MTG	R	21	55	−15	−14	4.3	459
Cb Lob VI Hem	R		9	−66	−16	4.41	729
Cb Lob VIIa Hem	L		−43	−66	−16	3.67	405
Cb Lob VIIa Hem	R		46	−51	−25	5.5	594

ITG, inferior temporal gyrus; TTG, transverse temporal gyrus; PHC, parahippocampal gyrus; FG, fusiform gyrus.

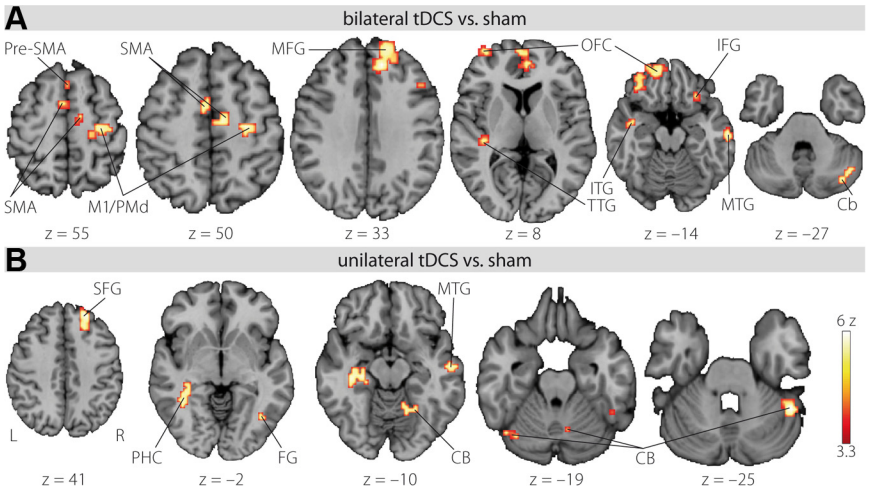

Fig. 5. Brain areas that showed a significant increase in eigenvector centrality after bilateral (*A*) and unilateral (*B*) tDCS over SM1 compared with sham stimulation. Significant clusters are presented on axial slices at a threshold of $z > 3.3$ ($P < 0.05$, corrected on cluster level). See also Table 3 for a detailed cluster list. OFC, orbitofrontal cortex; ITG, inferior temporal gyrus; TTG, transverse temporal gyrus; CB, cerebellum; PHC, parahippocampal cortex; FG, fusiform gyrus.

also in remote interconnected brain areas (Bestmann et al. 2004).

Other graph-theoretical analyses have been previously applied to investigate tDCS-induced neuroplastic changes. With the use of EEG (Polania et al. 2010) as well as fMRI (Polania et al. 2011b), it has been demonstrated that tDCS evokes intra- and interhemispheric connectivity changes after 10 min of stimulation over left M1. These effects were seen not only over the stimulated M1 but also in bilateral frontal, parietal, and premotor cortical regions (Polania et al. 2010). Furthermore, with the help of the higher spatial resolution in fMRI, it was demonstrated that 10 min of anodal tDCS over left SM1 increased short-range connections from M1 to premotor and parietal cortical regions, while concomitantly increasing interconnectedness in prefrontal cortex in resting brain dynamics (Polania et al. 2011b). Compared with our study, there are

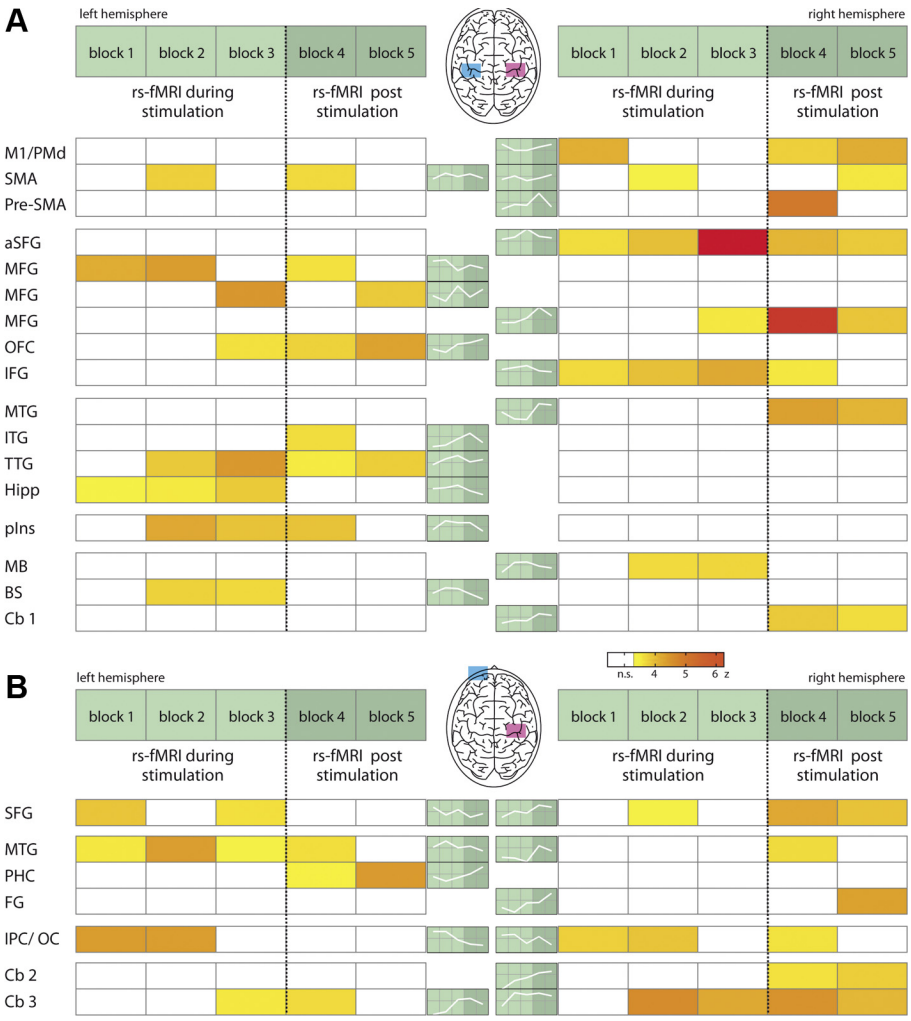

Fig. 6. Dynamic progression of changes in eigenvector centrality during (*blocks 1–3*) and after (*blocks 4* and *5*) bilateral (*A*) and unilateral (*B*) tDCS over SM1 compared with sham stimulation. Color-coded fields represent the z values resulting from the contrasts of a single block (*1–5*) and the baseline at a threshold of $z > 3.3$. During both conditions (*A* and *B*), distributed brain areas are modulated by tDCS. Note that the pattern of changes for both stimulation types seems to be nonlinear and temporally dispersed. The small line plots on green background represent continuous eigenvector centrality mapping (ECM) changes throughout the time course of the experiment and include below-threshold z values. Color bars indicate the z score in a range of 3.3–6.3; n.s., not significant. aSFG, anterior part of superior frontal gyrus; pIns, posterior insula; Cb, cerebellum, lobule VI.

some essential differences regarding the stimulation setup: Polania and colleagues used unilateral anodal tDCS of the left SM1, while in our study anodal tDCS was applied over the right SM1. Furthermore, the stimulation duration differed remarkably between the aforementioned studies (10 min in the study of Polania et al. vs. 20 min in our study). Despite methodological differences in these studies, tDCS in general seems to modulate widespread changes not only in local but also in distant brain areas.

Here we further extend previous work on tDCS-induced brain network changes by investigating two important issues. First, we provide novel evidence regarding dynamic online effects on large-scale networks during 20 min of tDCS. We chose this timescale to be consistent with relevant studies investigating behavioral effects of tDCS (e.g., Reis et al. 2009; Vines et al. 2008). Second, we provide evidence regarding differential tDCS effects induced by uni- and bilateral tDCS over SM1.

Effects of tDCS on functional connectivity during stimulation. During bilateral tDCS over SM1, we detected increases within a cluster covering right M1/PMd, e.g., the cortical area under the anodal electrode. Since a tDCS-related change in right M1/PMd was only elicited by bilateral (right anodal and left cathodal) and not unilateral (only right anodal) SM1 stimulation, it seems likely that not only the local facilitatory effect of the right anodal stimulation but also the additional cathodal (inhibitory) stimulation of the left SM1 contributed to this effect. As shown previously, cathodal tDCS leads to a decrease in corticospinal excitability, most likely through a hyperpolarization of the resting membrane potential, and/or through a modification of synaptic efficacy (Nitsche et al. 2005; Stagg and Nitsche 2011). Thus it is tempting to speculate that downregulation of left SM1 by cathodal tDCS results in a disinhibition of the interhemispheric inhibitory drive from the left to the right M1, which in turn causes the observed increase of eigenvector centrality of the homologous SM1. Alternatively, as shown recently in the somatosensory domain, a modulation of interhemispheric inhibitory interactions between primary somatosensory cortices might as well account for this effect (Ragert et al. 2011).

Since all subjects were right-handed, we cannot rule out that this effect might be due to a modulation of lateralized interhemispheric interactions between both M1 (Baumer et al. 2007). To elucidate this, further studies should investigate the effects of a converse stimulation setup. Nonetheless, our results raise the hypothesis that the previously reported superior effects of bilateral compared with unilateral right SM1 stimulation (Vines et al. 2008) are at least partly mediated by a modulation of functional connectivity in the right primary motor cortex.

Apart from eigenvector centrality changes in right SM1, bilateral tDCS over SM1 resulted in significant changes in secondary motor areas such as the premotor cortex (right PMd) and SMA. Previous animal and human studies showed that both areas are tightly interconnected with the stimulated SM1 (Civardi et al. 2001; Strick et al. 1998). Therefore, bilateral tDCS over SM1 might also result in changes within interconnected brain areas that are reflected by ECM. Similarly, remote effects of noninvasive brain stimulation in SMA have been successfully identified with the use of concurrent TMS over M1 and fMRI measurements (Bestmann et al. 2008).

In contrast to bilateral tDCS over SM1, no online changes in eigenvector centrality were found in SM1 or premotor areas during unilateral tDCS over SM1. The absence of unilateral tDCS effects in these areas was surprising and certainly requires further investigation. One important aspect of our experimental design is the fact that in the unilateral SM1 tDCS condition the right, nondominant motor cortex was the target area of anodal tDCS. This stimulation setup is consistent with the study by Vines and colleagues (Vines et al. 2008) that compared the effects of uni- and bilateral tDCS over the motor cortex on motor performance. With our experimental design we cannot rule out that different effects on functional connectivity would be observed if tDCS were applied over M1 of the dominant (left) hemisphere (Nitsche et al. 2003c), an issue that requires further investigation. In this vein, a recent study suggests that the dominance of the targeted motor cortex does differentially contribute to stimulation-induced aftereffects (Schade et al. 2012). Another important point with respect to this experimental condition pertains to the attachment of the cathodal electrode over the left supraorbital region. With our—well-established—stimulation setup it is not unlikely that a modulation of frontal activity by this electrode also contributes significantly to changes in functional connectivity that we observed on the whole-brain level.

Apart from the divergent results in SM1 and secondary motor areas, we observed changes in centrality in prefrontal areas during both uni- and bilateral tDCS over SM1. Studies in primates suggested that the prefrontal cortex is involved in motor control such as context-dependent movement selection (Matsumoto et al. 2003), supported by anatomical findings in macaques showing multisynaptic connections between prefrontal and premotor/motor cortex (Miyachi et al. 2005). Nevertheless, it still remains elusive whether centrality changes in prefrontal areas are directly related to a modulation of SM1 or rather reflect a general effect of tDCS on the resting-state network per se. Furthermore, as discussed above, in the unilateral SM1 tDCS condition it might be that the "reference" electrode attached to the contralateral supraorbital region also contributed at least partially to centrality changes within prefrontal areas that are in close spatial proximity to the electrode. At least for the bilateral SM1 tDCS condition, it is reasonable to assume that tDCS is capable of modulating the connectivity not only within adjacent, but also remote, brain areas such as the prefrontal cortex.

Interestingly, only unilateral facilitatory stimulation over right SM1, but not bilateral tDCS, with facilitatory right and inhibitory left SM1 stimulation induced an increase of centrality within the ipsilateral right cerebellum. Only recently could it be demonstrated that tDCS applied over the cerebellum modulates the overall inhibitory tone that exerts the cerebellum over the motor cortex (Galea et al. 2009). In our study it is tempting to speculate that the increase in centrality of the cerebellum during ipsilateral facilitation of SM1 might be mediated via facilitatory cerebrocerebellar interactions (Kelly and Strick 2003).

What is the potential meaning of the present study for future applications of tDCS in patient populations such as those with chronic stroke? The present data on healthy individuals certainly do not allow us to speculate as to whether one or the other setup might be more efficient in motor rehabilitation (Hummel et al. 2005; Lindenberg et al. 2010) but might help to

generate hypotheses for future studies. Given that we observed very different patterns of changes depending on the stimulation setup, it might be that patients who differ, e.g., in their lesion location might also differentially benefit from one stimulation setup or the other. Future studies need to address these questions in patient populations in order to identify benchmarks for the establishment of individualized adjuvant tDCS protocols in motor rehabilitation.

It remains noteworthy that a considerable part of the areas modulated by tDCS are not specifically related to motor planning or execution. Furthermore, in the unilateral SM1 stimulation condition we did not detect changes in eigenvector centrality within the stimulated cortex. Our results showing changes in remote regions induced by tDCS are in line with previous studies combining TMS and fMRI or PET. With this methodological approach, changes in activation (BOLD signal) in remote but interconnected regions have consistently been observed, even in the absence of significant changes in activity at the stimulation site (Bestmann et al. 2003, 2004; Bohning et al. 1999; Denslow et al. 2005). However, we applied well-established stimulation parameters (electrode size, stimulation intensity, stimulation duration; e.g., Vines et al. 2008). Thus we are confident that our results are, even though not specific to the motor system, specific to the tDCS conditions that were applied: bilateral and unilateral tDCS over primary sensorimotor cortices.

Dynamics of stimulation-induced centrality changes. Our study design using concurrent tDCS and high-resolution fMRI enabled us to continuously track changes in functional connectivity not only during but also after stimulation in order to unravel the dynamic processes of tDCS-induced neuroplasticity.

Here, covering both online effects and aftereffects of stimulation, we provide novel evidence that the pattern of tDCS-induced engagements of different neural networks is temporally dispersed. Previously, it was suggested that neuroplastic changes after the application of noninvasive brain stimulation protocols do not necessarily appear directly after the stimulation but may arise with a temporal delay. For example, after paired-associative stimulation (PAS), a specific form of noninvasive brain stimulation, functional changes in corticospinal excitability have been reported to appear after an interval of 20–30 min postintervention (Missitzi et al. 2011). The authors speculated that only after a latent interval might the optimal strengthening of the synaptic efficacy be consolidated and become apparent. It is tempting to translate this observation into the dynamic and diverse temporal onsets of functional resting-state changes as seen in our study. Along these lines, recent neuroimaging studies suggested that other plasticity-inducing interventions like motor sequence learning (Steele and Penhune 2010) or complex motor skill learning (Taubert et al. 2011) may result in not only steadily increasing (linear) brain alterations but, at least to some extent, also diverse, nonlinear dynamic changes within different brain areas.

Finally, the present study has some limitations. First, our method (ECM) relies on resting-state measurements of the BOLD signal; thus we do not have a behavioral measure that could prove the relevance of our stimulation protocols. Hence, we cannot directly claim that the effects that we observed are linked to behavioral consequences of tDCS. However, we used an established and frequently tested stimulation setup known to improve motor performance and learning (see e.g., Nitsche et al. 2003c; Vines et al. 2008). Here we aimed to study changes in functional connectivity elicited by these established stimulation protocols. Therefore, our study should be considered in line with previous studies that explored neurophysiological effects of tDCS in the absence of a behavioral task (e.g., Nitsche et al. 2003a; Nitsche and Paulus 2000; Polania et al. 2011b; Zheng et al. 2011). Second, by using rs-fMRI and a data-driven analysis approach (ECM), we certainly cannot claim to provide a complete picture of tDCS-induced connectivity changes. However, the scope of the present study was to obtain a global picture of tDCS-induced functional connectivity changes without hypotheses about special brain regions. To further elucidate the specific involvement of certain brain regions, such as the stimulated M1, more hypothesis-driven approaches should address these issues in future studies. Third, to avoid any potential bias from baseline differences in ECM between conditions (sham, bilateral, and unilateral tDCS over SM1) we normalized the ECM maps during and after tDCS against baseline. This analysis is in line with a recently published study investigating aftereffects of tDCS over the dorsolateral prefrontal cortex. Since we found in an additional analysis that baseline ECM maps were in fact different between conditions, the possibility remains that baseline differences per se might have influenced the tDCS-induced ECM changes. Similar findings have been reported in recent noninvasive brain stimulation studies, a phenomenon known as homeostatic plasticity (Ziemann and Siebner 2008). More specifically, we cannot entirely rule out the possibility that the individual preinterventional state might have had an impact on subsequent tDCS-induced ECM changes. The impact of homeostatic plasticity on ECM changes should therefore be of interest in future investigations.

In the present study, we did not record respiration and heartbeat to model physiological noise. Therefore, we cannot rule out the possibility that these parameters might influence our research findings. However, a previous study investigated the influence of these parameters on rs-fMRI data and highlighted that default-mode network changes cannot be explained by cardiorespiratory processes alone and are likely related to cognitive neuronal processing (van Buuren et al. 2009). Therefore, we are confident that the observed tDCS-induced ECM changes are not contaminated by physiological noise.

In summary, we have demonstrated that tDCS over SM1 induces widespread and dynamic changes in resting-state functional connectivity both during and after stimulation. The pattern of network connectivity changes is temporally and spatially dispersed and critically depends on the stimulation setup (unilateral and bilateral tDCS over SM1).

DISCLOSURES

No conflicts of interest, financial or otherwise, are declared by the author(s).

AUTHOR CONTRIBUTIONS

Author contributions: B.S., D.M., A.V., and P.R. conception and design of research; B.S., M.T., and P.R. performed experiments; B.S., A.S., J.K., D.M., and V.C. analyzed data; B.S., A.S., J.K., D.M., V.C., M.T., A.V., and P.R. interpreted results of experiments; B.S., A.S., and J.K. prepared figures; B.S., V.C., and M.T. drafted manuscript; B.S., A.S., J.K., D.M., V.C., M.T., A.V., and P.R. edited and revised manuscript; B.S., A.S., J.K., D.M., V.C., M.T., A.V., and P.R. approved final version of manuscript.

REFERENCES

Achard S, Salvador R, Whitcher B, Suckling J, Bullmore E. A resilient, low-frequency, small-world human brain functional network with highly connected association cortical hubs. *J Neurosci* 26: 63–72, 2006.

Alon G, Roys SR, Gullapalli RP, Greenspan JD. Non-invasive electrical stimulation of the brain (ESB) modifies the resting-state network connectivity of the primary motor cortex: a proof of concept fMRI study. *Brain Res* 1403: 37–44, 2011.

Antal A, Polania R, Schmidt-Samoa C, Dechent P, Paulus W. Transcranial direct current stimulation over the primary motor cortex during fMRI. *Neuroimage* 55: 590–596, 2011.

Baudewig J, Nitsche MA, Paulus W, Frahm J. Regional modulation of BOLD MRI responses to human sensorimotor activation by transcranial direct current stimulation. *Magn Reson Med* 45: 196–201, 2001.

Baumer T, Dammann E, Bock F, Kloppel S, Siebner HR, Munchau A. Laterality of interhemispheric inhibition depends on handedness. *Exp Brain Res* 180: 195–203, 2007.

Bestmann S, Baudewig J, Siebner HR, Rothwell JC, Frahm J. Subthreshold high-frequency TMS of human primary motor cortex modulates interconnected frontal motor areas as detected by interleaved fMRI-TMS. *Neuroimage* 20: 1685–1696, 2003.

Bestmann S, Baudewig J, Siebner HR, Rothwell JC, Frahm J. Functional MRI of the immediate impact of transcranial magnetic stimulation on cortical and subcortical motor circuits. *Eur J Neurosci* 19: 1950–1962, 2004.

Bestmann S, Ruff CC, Blankenburg F, Weiskopf N, Driver J, Rothwell JC. Mapping causal interregional influences with concurrent TMS-fMRI. *Exp Brain Res* 191: 383–402, 2008.

Bohning DE, Shastri A, McConnell KA, Nahas Z, Lorberbaum JP, Roberts DR, Teneback C, Vincent DJ, George MS. A combined TMS/fMRI study of intensity-dependent TMS over motor cortex. *Biol Psychiatry* 45: 385–394, 1999.

Bonacich P. Some unique properties of eigenvector centrality. *Social Netw* 29: 555–564, 2007.

Civardi C, Cantello R, Asselman P, Rothwell JC. Transcranial magnetic stimulation can be used to test connections to primary motor areas from frontal and medial cortex in humans. *Neuroimage* 14: 1444–1453, 2001.

Denslow S, Lomarev M, George MS, Bohning DE. Cortical and subcortical brain effects of transcranial magnetic stimulation (TMS)-induced movement: an interleaved TMS/functional magnetic resonance imaging study. *Biol Psychiatry* 57: 752–760, 2005.

Forman SD, Cohen JD, Fitzgerald M, Eddy WF, Mintun MA, Noll DC. Improved assessment of significant activation in functional magnetic resonance imaging (fMRI): use of a cluster-size threshold. *Magn Reson Med* 33: 636–647, 1995.

Fox MD, Raichle ME. Spontaneous fluctuations in brain activity observed with functional magnetic resonance imaging. *Nat Rev Neurosci* 8: 700–711, 2007.

Fritsch B, Reis J, Martinowich K, Schramba HM, Ji Y, Cohen LG, Lu B. Direct current stimulation promotes BDNF-dependent synaptic plasticity: potential implications for motor learning. *Neuron* 66: 198–204, 2010.

Galea JM, Jayaram G, Ajagbe L, Celnik P. Modulation of cerebellar excitability by polarity-specific noninvasive direct current stimulation. *J Neurosci* 29: 9115–9122, 2009.

Gandiga PC, Hummel FC, Cohen LG. Transcranial DC stimulation (tDCS): a tool for double-blind sham-controlled clinical studies in brain stimulation. *Clin Neurophysiol* 117: 845–850, 2006.

He Y, Wang J, Wang L, Chen ZJ, Yan C, Yang H, Tang H, Zhu C, Gong Q, Zang Y, Evans AC. Uncovering intrinsic modular organization of spontaneous brain activity in humans. *PLoS One* 4: e5226, 2009.

Holland R, Leff AP, Josephs O, Galea JN, Desikan M, Price CJ, Rothwell JC, Crinion J. Speech facilitation by left inferior frontal cortex stimulation. *Curr Biol* 21: 1403–1407, 2011.

Hummel F, Celnik P, Giraux P, Floel A, Wu WH, Gerloff C, Cohen LG. Effects of non-invasive cortical stimulation on skilled motor function in chronic stroke. *Brain* 128: 490–499, 2005.

Isaacs KL, Barr WB, Nelson PK, Devinsky O. Degree of handedness and cerebral dominance. *Neurology* 66: 1855–1858, 2006.

Keeser D, Meindl T, Bor J, Palm U, Pogarell O, Mulert C, Brunelin J, Möller HJ, Reiser M, Padberg E. Prefrontal transcranial direct current stimulation changes connectivity of resting-state networks during fMRI. *J Neurosci* 31: 15284–15293, 2011.

Kelly RM, Strick PL. Cerebellar loops with motor cortex and prefrontal cortex of a nonhuman primate. *J Neurosci* 23: 8432–8444, 2003.

Kirimoto H, Ogata K, Onishi H, Oyama M, Goto Y, Tobimatsu S. Transcranial direct current stimulation over the motor association cortex induces plastic changes in ipsilateral primary motor and somatosensory cortices. *Clin Neurophysiol* 122: 777–783, 2011.

Kwon YH, Jang SH. The enhanced cortical activation induced by transcranial direct current stimulation during hand movements. *Neurosci Lett* 492: 105–108, 2011.

Lang N, Siebner HR, Ward NS, Lee L, Nitsche MA, Paulus W, Rothwell JC, Lemon RN, Frackowiak RS. How does transcranial DC stimulation of the primary motor cortex alter regional neuronal activity in the human brain? *Eur J Neurosci* 22: 495–504, 2005.

Lindenberg R, Renga V, Zhu LL, Nair D, Schlaug G. Bihemispheric brain stimulation facilitates motor recovery in chronic stroke patients. *Neurology* 75: 2176–2184, 2010.

Lohmann G, Margulies DS, Horstmann A, Pleger B, Lepsien J, Goldhahn D, Schloegl H, Stumvoll M, Villringer A, Turner R. Eigenvector centrality mapping for analyzing connectivity patterns in FMRI data of the human brain. *PLoS One* 5: e10232, 2010.

Lohmann G, Muller K, Bosch V, Mentzel H, Hessler S, Chen L, Zysset S, von Cramon DY. LIPSIA—a new software system for the evaluation of functional magnetic resonance images of the human brain. *Comput Med Imaging Graph* 25: 449–457, 2001.

Matsumoto K, Suzuki W, Tanaka K. Neuronal correlates of goal-based motor selection in the prefrontal cortex. *Science* 301: 229–232, 2003.

Missitzi J, Gentner R, Geladas N, Karandreas N, Classen J, Klissouras V. Plasticity in human motor cortex is in part genetically determined. *J Physiol* 589: 297–306, 2011.

Miyachi S, Lu X, Inoue S, Iwasaki T, Koike S, Nambu A, Takada M. Organization of multisynaptic inputs from prefrontal cortex to primary motor cortex as revealed by retrograde transneuronal transport of rabies virus. *J Neurosci* 25: 2547–2556, 2005.

Neuling T, Rach S, Wagner S, Wolters CH, Herrmann CS. Good vibrations: oscillatory phase shapes perception. *Neuroimage* 63: 771–778, 2012.

Nitsche MA, Cohen LG, Wassermann EM, Priori A, Lang N, Antal A, Paulus W, Hummel F, Boggio PS, Fregni F, Pascual-Leone A. Transcranial direct current stimulation: state of the art 2008. *Brain Stimul* 1: 206–223, 2008.

Nitsche MA, Fricke K, Henschke U, Schitterlau A, Liebetanz D, Lang N, Henning S, Tergau F, Paulus W. Pharmacological modulation of cortical excitability shifts induced by transcranial direct current stimulation in humans. *J Physiol* 553: 293–301, 2003a.

Nitsche MA, Liebetanz D, Lang N, Antal A, Tergau F, Paulus W. Safety criteria for transcranial direct current stimulation (tDCS) in humans. *Clin Neurophysiol* 114: 2220–2222, 2003b.

Nitsche MA, Paulus W. Excitability changes induced in the human motor cortex by weak transcranial direct current stimulation. *J Physiol* 527: 633–639, 2000.

Nitsche MA, Schauenburg A, Lang N, Liebetanz D, Exner C, Paulus W, Tergau F. Facilitation of implicit motor learning by weak transcranial direct current stimulation of the primary motor cortex in the human. *J Cogn Neurosci* 15: 619–626, 2003c.

Nitsche MA, Seeber A, Frommann K, Klein CC, Rochford C, Nitsche MS, Fricke K, Liebetanz D, Lang N, Antal A, Paulus W, Tergau F. Modulating parameters of excitability during and after transcranial direct current stimulation of the human motor cortex. *J Physiol* 568: 291–303, 2005.

Oldfield RC. The assessment and analysis of handedness: the Edinburgh inventory. *Neuropsychologia* 9: 97–113, 1971.

Pena-Gomez C, Sala-Lonch R, Junque C, Clemente IC, Vidal D, Bargallo N, Falcon C, Valls-Sole J, Pascual-Leone A, Bartres-Faz D. Modulation of large-scale brain networks by transcranial direct current stimulation evidenced by resting-state functional MRI. *Brain Stimul* 5: 252–263, 2012.

Polania R, Nitsche MA, Paulus W. Modulating functional connectivity patterns and topological functional organization of the human brain with transcranial direct current stimulation. *Hum Brain Mapp* 32: 1236–1249, 2011a.

Polania R, Paulus W, Antal A, Nitsche MA. Introducing graph theory to track for neuroplastic alterations in the resting human brain: a transcranial direct current stimulation study. *Neuroimage* 54: 2287–2296, 2011b.

Ragert P, Nierhaus T, Cohen LG, Villringer A. Interhemispheric interactions between the human primary somatosensory cortices. *PLoS One* 6: e16150, 2011.

Ragert P, Vandermeeren Y, Camus M, Cohen LG. Improvement of spatial tactile acuity by transcranial direct current stimulation. *Clin Neurophysiol* 119: 805–811, 2008.

Reis J, Robertson EM, Krakauer JW, Rothwell J, Marshall L, Gerloff C, Wassermann E, Pascual-Leone A, Hummel F, Celnik PA, Classen J, Floel A, Ziemann U, Paulus W, Siebner HR, Born J, Cohen LG. Consensus: can transcranial direct current stimulation and transcranial magnetic stimulation enhance motor learning and memory formation? *Brain Stimul* 1: 363–369, 2008.

Reis J, Schambra HM, Cohen LG, Buch ER, Fritsch B, Zarahn E, Celnik PA, Krakauer JW. Noninvasive cortical stimulation enhances motor skill acquisition over multiple days through an effect on consolidation. *Proc Natl Acad Sci USA* 106: 1590–1595, 2009.

Rubinov M, Sporns O. Complex network measures of brain connectivity: uses and interpretations. *Neuroimage* 52: 1059–1069, 2010.

Schade S, Moliadze V, Paulus W, Antal A. Modulating neuronal excitability in the motor cortex with tDCS shows moderate hemispheric asymmetry due to subjects' handedness: a pilot study. *Restor Neurol Neurosci* 30: 191–198, 2012.

Stagg CJ, Best JG, Stephenson MC, O'Shea J, Wylezinska M, Kincses ZT, Morris PG, Matthews PM, Johansen-Berg H. Polarity-sensitive modulation of cortical neurotransmitters by transcranial stimulation. *J Neurosci* 29: 5202–5206, 2009.

Stagg CJ, Jayaram G, Pastor D, Kincses ZT, Matthews PM, Johansen-Berg H. Polarity and timing-dependent effects of transcranial direct current stimulation in explicit motor learning. *Neuropsychologia* 49: 800–804, 2011.

Stagg CJ, Nitsche MA. Physiological basis of transcranial direct current stimulation. *Neuroscientist* 17: 37–53, 2011.

Steele CJ, Penhune VB. Specific increases within global decreases: a functional magnetic resonance imaging investigation of five days of motor sequence learning. *J Neurosci* 30: 8332–8341, 2010.

Strick PL, Dum RP, Picard N. Motor areas on the medial wall of the hemisphere. *Novartis Found Symp* 218: 64–75, 1998.

Taubert M, Lohmann G, Margulies DS, Villringer A, Ragert P. Long-term effects of motor training on resting-state networks and underlying brain structure. *Neuroimage* 57: 1492–1498, 2011.

van Buuren M, Gladwin TE, Zandbelt BB. Cardiorespiratory effects on default-mode network activity as measured with fMRI. *Hum Brain Mapp* 30: 3031–3042, 2009.

van der Werf YD, Sanz-Arigita EJ, Menning S, van den Heuvel OA. Modulating spontaneous brain activity using repetitive transcranial magnetic stimulation. *BMC Neurosci* 11: 145, 2010.

Venkatakrishnan A, Sandrini M. Combining transcranial direct current stimulation and neuroimaging: novel insights in understanding neuroplasticity. *J Neurophysiol* 107: 1–4, 2012.

Vines BW, Cerruti C, Schlaug G. Dual-hemisphere tDCS facilitates greater improvements for healthy subjects' non-dominant hand compared to uni-hemisphere stimulation. *BMC Neurosci* 9: 103, 2008.

Zheng X, Alsop DC, Schlaug G. Effects of transcranial direct current stimulation (tDCS) on human regional cerebral blood flow. *Neuroimage* 58: 26–33, 2011.

Ziemann U, Siebner HR. Modifying motor learning through gating and homeostatic metaplasticity. *Brain Stimul* 1: 60–66, 2008.

Zuo XN, Ehmke R, Mennes M, Imperati D, Castellanos FX, Sporns O, Milham MP. Network centrality in the human functional connectome. *Cereb Cortex* 22: 1862–1875, 2012.